Desalination and Water Treatment
www.deswater.com
doi: 10.1080/19443994.2015.1008050

57 (2016) 6365–6371
March

Taylor & Francis
Taylor & Francis Group

Study the photocatalysis activity of hydrothermal-synthesized $BiVO_4$–graphene composite on methylene blue

Xiang Cai[a], Bing Zhang[b], Lei Shi[b], Huidi Liu[b], Jinglin Zhang[b], Langhuan Huang[b], Shaozao Tan[b,*]

[a]*Department of Light Chemical Engineering, Guangdong Polytechnic, Foshan 528041, P.R. China, Tel. +86 757 83106906; email: cecaixiang@163.com*
[b]*Department of Chemistry, Jinan University, Guangzhou 510632, P.R. China, Tel./Fax: +86 20 85223670; emails: mana1@qq.com (B. Zhang), 1101465969@qq.com (L. Shi), liuhdjy@163.com (H. Liu), tjnujlzhang@163.com (J. Zhang), thuanglh@jnu.edu.cn (L. Huang), tanshaozao@163.com (S. Tan)*

Received 30 May 2014; Accepted 7 January 2015

ABSTRACT

A hydrothermal synthesis method was developed to prepare graphene-supported bismuth vanadate ($BiVO_4$) particle ($BiVO_4$–graphene) using graphene oxide, $Bi(NO_3)_3{\cdot}5H_2O$, and NH_4VO_3 as raw materials. The composite was characterized by various analytical methods, including X-ray powder diffraction, Fourier transform infrared spectroscopy, diffuse reflection spectra, transmission electron microscope, X-ray photoelectron emission spectroscopy, and fluorescence spectra. The photocatalytic activity of $BiVO_4$–graphene composite was investigated by the degradation of methylene blue in an aqueous solution under visible light irradiation. It had been confirmed that the presence of graphene enhanced the photocatalytic activity of $BiVO_4$ particle, and the $BiVO_4$–1.0% graphene showed the best photocatalytic activity. The improved visible light activity of $BiVO_4$–graphene was due to the enhancement of electron–hole separation by the electron trapping of graphene. Also, a possible mechanism was proposed to elucidate the role of graphene in $BiVO_4$–graphene composite as a photocatalyst for degradation of organic pollutant.

Keywords: Bismuth vanadate; Graphene; Photocatalysis; Visible light; Electron trapping

1. Introduction

Photocatalysis over semiconductor using solar energy has attracted extensive attention in splitting of water and the degradation of organic pollutant [1,2]. In recent years, bismuth vanadate ($BiVO_4$) has been demonstrated to be a good visible-light-driven photocatalyst with narrow gap energy of 2.4 eV [3,4]. $BiVO_4$ has three crystallographic forms: tetragonal zircon, tetragonal scheelite, and monoclinic scheelite. It has been reported that monoclinic form is more photocatalytically active than other forms under visible light irradiation [5,6]. However, the performance of pure $BiVO_4$ in photocatalytic degradation of organic pollutant is somewhat limited by its poor adsorptive performance and difficulty in migration of photogenerated electron–hole pairs [3,5]. To resolve this problem, a variety of strategies have been proposed to improve the photocatalytic performance of $BiVO_4$, such as suitable textural design [7], non-metal doping

*Corresponding author.

1944-3994/1944-3986 © 2015 Balaban Desalination Publications. All rights reserved.

[8], noble metal deposition [3,5,9,10], and constructing heterojunction between semiconductors [11].

Graphene, a two-dimensional crystal which is made up of sp^2-hybrisized carbon atoms, has received significant attention in both the experimental and the theoretical scientific fields due to its outstanding mechanical, electrical, thermal, and optical properties [12–14]. Especially, high thermal conductivity (~5,000 W m^{-1} K^{-1}) [15], excellent mobility of charge carrier (200,000 cm^{-1} V^{-1} s^{-1}) [16], and large theoretical specific area (~2,600 m^2 g^{-1}) [17] properties make graphene attractive for many practical applications, such as batteries [18], sensors [19], capacitors [20], and catalytic fields [21]. Graphene is easy to obtain from inexpensive graphite via intermediate product "graphene oxide" [22,23]. Graphene oxide contains a range of reactive oxygen functional on the sheet surface, which makes it act as an excellent support for various graphene-based composites. Recently, graphene-based semiconductor photocatalyst is of great interest due to its good electron conductivity, large specific surface area, and high adsorption [24–26]. Kamat and co-workers [24,26,27] reported TiO_2/graphene oxide nanocrystalline composite and testified the possibility of using graphene as an electron acceptor for reducing the recombination of the photogenerated electron–hole pair in the graphene/TiO_2 composite photocatalyst, which had attracted tremendous attention. Li et al. [28] synthesized CdS–graphene nanocomposite by a solvothermal method. They found that the nanocomposite enhanced the hydrogen production rate when compared to the pure CdS nanoparticle. Xiang et al. [29] synthesized C_3N_4–graphene nanocomposite by a combined impregnation-chemical reduction method. The results showed that the metal-free C_3N_4–graphene composite showed high visible-light photocatalytic activity. Obviously, graphene is a promising material for exploitation of high-performance photocatalyst. Considering the intrinsic properties of $BiVO_4$ and graphene, it is expected that the combination of $BiVO_4$ with graphene may be an ideal system with excellent photocatalysis performance.

Herein, we presented an easy and general method to prepare $BiVO_4$–graphene composite by a hydrothermal reaction using graphene oxide, $Bi(NO_3)_3{\cdot}5H_2O$, and NH_4VO_3 as raw materials. The structure and the property of composite were investigated. Furthermore, the $BiVO_4$–graphene composite was demonstrated to have great potential as an effective material for removing dye pollutant in water. Also, a possible mechanism was proposed to elucidate the role of graphene in $BiVO_4$–graphene composite as a photocatalyst for degradation of organic pollutant.

2. Experimental

2.1. Preparation of $BiVO_4$–graphene composite

All chemicals were of analytical grade and were used without further purification. Deionized water was used in all experiments. Graphene oxide was prepared from graphite powders through the modified Hummers' method [22]. A typical preparation of $BiVO_4$–graphene composite was described as follows: 0.005 mol $Bi(NO_3)_3{\cdot}5H_2O$ and 0.005 mol NH_4VO_3 were separately dissolved in 20 mL of 35% (w/w) HNO_3 and 20 mL 6 mol/L NaOH solution, and each of them was stirred for 30 min at room temperature. A varying amount of graphene oxide solution (0.5 mg/mL) was added to the $Bi(NO_3)_3$ aqueous solution slowly and stirred for 1 h. After that these two mixtures were mixed together and stirred for 3 h. Next, the homogeneous suspension was transferred into a 50 mL teflon-lined stainless steel autoclave and heated at 180˚C for 12 h. After cooling to room temperature, the product was washed with distilled water for three times, and then dried under air at 60˚C. The obtained sample was denoted as $BiVO_4$–graphene composite.

2.2. Analytical methods

The powder X-ray diffraction (XRD) patterns were recorded by an X-ray diffractometer (MSAL-XD) using a Cu Kα radiation. The transmission electron microscope (TEM) investigations were taken on a PHILIPS TECNAI-10 microscope and JEOL JEM-2010 (HR) microscope. The diffuse reflection spectra (DRS) were determined by a SHIMADZU-2501PC spectrometer equipped with integrating sphere accessory. The fluorescence spectra (FL) were recorded on an F-4500 HITACHI fluorometry. The X-ray photoelectron spectroscopy (XPS) measurements were performed on a THERMO ELECTRON ESCALAB-250 spectrometer with an Al Kα emission as the X-ray source.

2.3. Evaluation of photocatalytic activity

The photocatalytic experiments were carried out in a XUJIANG XPA-2 photochemical reactor. The reaction suspension was prepared by adding 0.100 g of catalyst into a 100 mL of aqueous methylene blue (MB) solution with an initial concentration of 5 mg/L. Prior to photodegradation, the suspension was magnetically stirred in darkness for 30 min to establish an adsorption and desorption equilibrium. The suspension containing MB and catalyst was irradiated by a 500 w xenon lamp. The cut-off filter (HITACHI Y-430) was used to obtain visible light ($\lambda > 420$ nm). The

concentration of MB solution was quantified by a TU-1900 spectrophotometer at 662 nm. To investigate the active oxidative species generated in the photocatalytic process, the radicals and holes trapping experiments were studied. The formic acid (FA), a commonly used hole scavenger and tert-butyl alcohol (TBA), a hydroxyl radical scavenger, were added into the solution, respectively.

3. Results and discussion

3.1. XRD analysis

The XRD patterns of graphene, $BiVO_4$, and $BiVO_4$–graphene composites with different contents of graphene were shown in Fig. 1. For graphene, the peak at $2\theta = 24.8^{\circ}$, represents the (0 0 2) interlayer spacing of 0.359 nm (Fig. 1(a)). This value is slightly larger than that of graphite, which is mainly due to the residual functional groups that may exist between the rGO layers. For $BiVO_4$ (Fig. 1(b)), almost all the diffraction peaks can be assigned to monoclinic $BiVO_4$ (JCPDS 14-0688), which exhibits the most active photocatalysis under visible light irradiation. The XRD patterns of $BiVO_4$–graphene samples almost coincided with that of pure $BiVO_4$. Noticeably, the peaks for graphene were not observed in the diffraction patterns of $BiVO_4$–graphene composites. The reason could be ascribed to low amount and relatively low diffraction intensity of graphene.

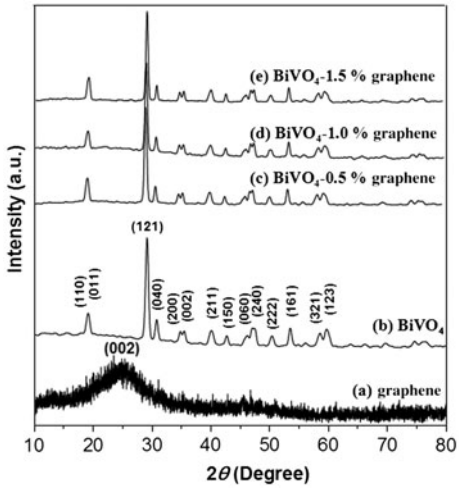

Fig. 1. XRD patterns of the (a) graphene, (b) pure $BiVO_4$, (c) $BiVO_4$–0.5% graphene, (d) $BiVO_4$–1.0% graphene, and (e) $BiVO_4$–1.5% graphene.

3.2. TEM analysis

The images of $BiVO_4$ particles and $BiVO_4$–1.0% graphene composite were shown in Fig. 2. Image of pure $BiVO_4$ particles showed that the particles were mostly aggregated. The image of $BiVO_4$–1.0% graphene demonstrated that $BiVO_4$ particles were successfully deposited on graphene. Besides, most of $BiVO_4$ particles were dispersed.

3.3. Fourier transform infrared and XPS analysis

Fig. 3(a) shows the Fourier transform infrared (FTIR) spectra of $BiVO_4$, graphene oxide, and $BiVO_4$–1.0% graphene composite. It was demonstrated that a large quantities of oxygen-containing functional groups existed in the forms of epoxy, hydroxyl, and carboxyl groups on the surface of graphene oxide. The broad absorption at 3,200–3,400 cm^{-1} was due to the O–H stretching vibration; the peak at 1,721 cm^{-1} could be assigned to the C=O stretching vibration; 1,622 cm^{-1} was ascribed to H–O–H bending of water; the bands at 1,407, 1,223, 1,048, and 987 cm^{-1} were, respectively, correspond to stretching vibrations of the tertiary alcoholic C–OH stretching, phenolic C–OH stretching, C–O stretching, and epoxy stretching [30,31]. However, all these bands related with the oxygen-containing functional groups in the FTIR spectrum of $BiVO_4$–1% graphene composite were removed, indicating considerable reduction of graphene oxide or the low quantity of graphene oxide in the composite. It was interesting to note that the V–O vibration of $BiVO_4$ shifted from 743 to 738 cm^{-1}, suggesting the interaction between $BiVO_4$ and graphene perturbed the V–O bond [32]. Furthermore, XPS was performed to illustrate the reduction of GO in $BiVO_4$–graphene composite. Fig. 3(b) shows the deconvoluted XPS C1s spectra of $BiVO_4$–1% graphene composite. It was clearly seen that there were four types of carbon bonds: C–C (284.79 eV), C–OH (286.32 eV), C=O (287.29 eV), and O=C–OH (288.27 eV) [33,34]. The peak intensities of oxygen-containing functional groups were very low, which revealed that most of oxygen-containing functional groups were removed after the hydrothermal reaction at 180°C for 12 h.

3.4. DRS analysis

Fig. 4 shows the diffuse reflection of $BiVO_4$–graphene composite. For comparison, pure $BiVO_4$ was also evaluated. The absorption edge of pure $BiVO_4$ was about 552 nm, so the band gap energy of $BiVO_4$ could be estimated to be 2.24 eV. Compared with that of $BiVO_4$, the absorption edge of $BiVO_4$–graphene

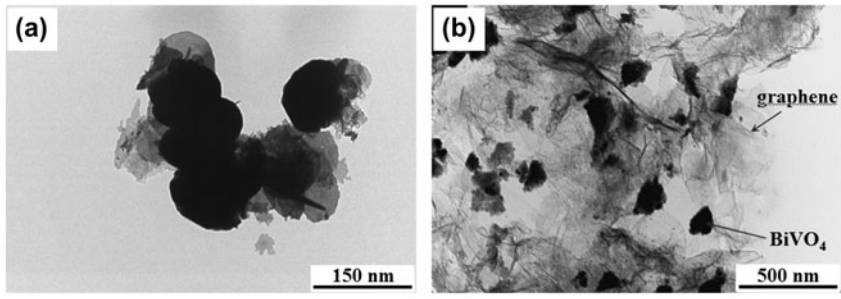

Fig. 2. TEM of (a) pure $BiVO_4$ and (b) $BiVO_4$–1.0% graphene.

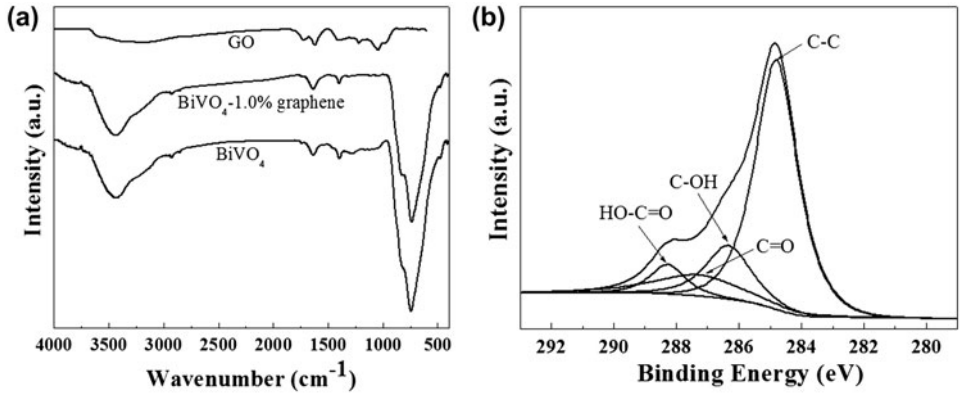

Fig. 3. (a) FTIR spectra of $BiVO_4$, graphene oxide and $BiVO_4$–1.0% graphene and (b) C1s XPS of $BiVO_4$–1.0% graphene.

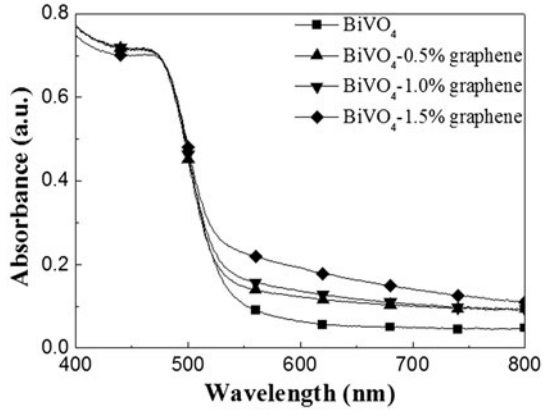

Fig. 4. UV–vis diffuses reflectance spectra of $BiVO_4$–graphene composites.

composite did not shift towards the longer wavelength, but the absorbance intensity in the visible range was increased with the increase in graphene content. The increase in absorption in the visible light region could be ascribed to the presence of carbon in the $BiVO_4$–graphene composite which reduced the reflection of light. Because of the increase of absorption in the visible light region, the solar energy could be more efficiently used.

3.5. Photoluminescence emission analysis

The photoluminescence emission (PL) spectra were used to investigate the separation efficiency of electron–hole pairs. As shown in Fig. 5, the PL intensity of $BiVO_4$–graphene composite was lower than that of $BiVO_4$, and decreased with the decrease in graphene content. The PL signals were attributed to the radiative recombination process of self-trapped excitons [35,36]. So the decrease of PL intensity indicated the enhancement of separation efficiency of electron–hole pairs. While the electron formed by the visible light irradiation was migrated to the surface of $BiVO_4$, it was trapped by graphene. Thus, the high rate of electron–hole recombination, which decreased the quantum yield of the photocatalytic process, could be declined. The experimental results demonstrated that the separation efficiency of electron–hole pairs was sensitive to the loading of graphene.

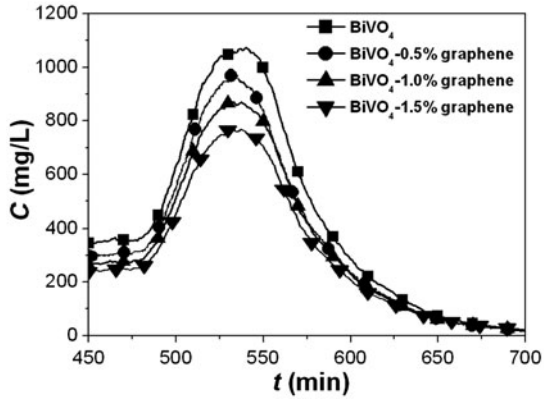

Fig. 5. The PL spectra of pure $BiVO_4$ and $BiVO_4$–1.0% graphene.

3.6. Photocatalytic efficiency

The photocatalytic efficiency was evaluated by the photodegradation of MB in an aqueous solution under visible light irradiation. Fig. 6(a) shows the photodegradation results over various $BiVO_4$–graphene composites. It was clearly seen that the pure $BiVO_4$ exhibited relatively low degradation efficiency (Fig. 6(a)), which was ascribed to the poor adsorptive performance and difficulty in migration of electron–hole pairs of pure $BiVO_4$. The visible light activity had been enhanced when graphene was introduced in the $BiVO_4$ particles. The experimental results showed with the increase of ratio between graphene and $BiVO_4$, the photodegradation ratio of MB was increased initially. However, the photodegradation ratio of MB was decreased when the graphene content exceeded 1.0 wt.%. It implied that there was an optimum content of graphene. For $BiVO_4$–graphene composite under visible light irradiation, $BiVO_4$ was excited and generated holes and electrons, and graphene as an acceptor of electrons could quickly trap electrons. This could enhance the separation efficiency of electron-hole pairs, leaving more charge carriers to participate the oxidation reaction and promote the degradation of MB. When the graphene content exceeded 1.0 wt.%, we suggest that the graphene will be stacking together via π-π interaction, which will reduce the electrons trapability, and decrease the degradation of MB.

In order to identify the reactive species generated in the photocatalytic degradation process, the trapping experiments of holes and radicals were studied. Fig. 6(b) shows the photodegradation of MB with the additions of hole and hydroxyl radical scavengers, respectively. The experimental results demonstrated that after FA (a commonly used holes scavenger) was added into the solution, the photocatalytic degradation of MB was fully restrained, while the photocatalytic degradation of MB had not been obviously changed after the addition of TBA (a hydroxyl radical scavenger). This indicated that the hydroxyl radical was not the main active oxidative specie in the photocatalytic reaction, but the photocatalytic process was mainly mastered by the oxidation of hole.

From all experimental results mentioned above, a possible mechanism for photodegradation of MB over $BiVO_4$–graphene composite had been investigated as illustrated in Fig. 7. Under visible light irradiation, $BiVO_4$ was excited and generated holes and electrons (1). Without introduction of graphene, electrons would quickly transition from CB to VB and then recombine with holes, resulting in a low photocatalytic degradation performance. After introduction of graphene in the $BiVO_4$–graphene system, graphene served as an acceptor of the electrons generated in $BiVO_4$ surface (2), thus the probability of electron-hole recombination would decrease. These electrons could contact oxygen molecules to produce superoxide anion radical (3), meanwhile the holes might react with the OH^-

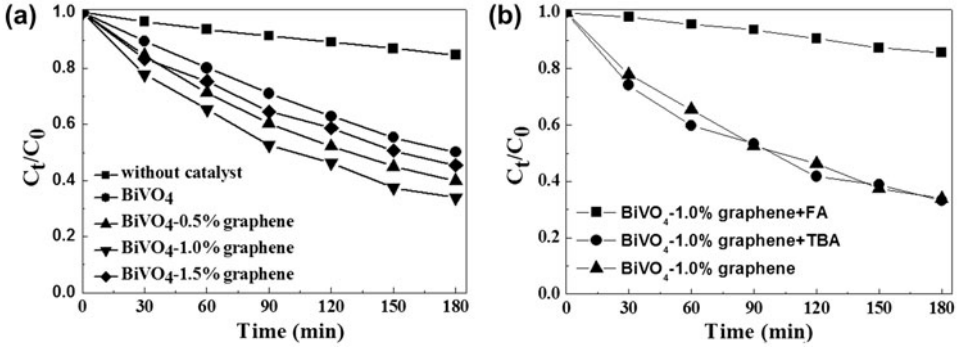

Fig. 6. (a) Photocatalytic degradation of MB over various $BiVO_4$–graphene composites and (b) photocatalytic degradation of MB over $BiVO_4$–1.0% graphene with the addition of FA and TBA.

$$BiVO_4 + hv \longrightarrow BiVO_4 (h^+_{VB} + e^-_{CB}) \quad \text{(Eq. 1)}$$

$$BiVO_4 (e) + \text{graphene} \longrightarrow BiVO_4 + \text{graphene} (e) \quad \text{(Eq. 2)}$$

$$\text{graphene} (e) + O_2 \longrightarrow O_2^{\cdot -} + \text{graphene} \quad \text{(Eq. 3)}$$

$$BiVO_4 (h) + OH^- \longrightarrow BiVO_4 + {}^{\cdot}OH \quad \text{(Eq. 4)}$$

Fig. 7. A possible mechanism of the enhancement of photocatalytic activity of $BiVO_4$ by introduction of graphene under visible light irradiation.

derived from H_2O and form a hydroxyl radical $^{\cdot}OH$ (4). From the above discussion, we could confer that the MB molecule could be photocatalytically decomposed to CO_2 and H_2O by oxygen peroxide radical $O_2^{\cdot -1}$ and hydroxyl radical $^{\cdot}OH$ [37].

4. Conclusion

Using graphene oxide as a support, we developed a hydrothermal method to prepare $BiVO_4$–graphene composite. The morphology and structure of the composite were extensively investigated by XRD, TEM, FTIR, DRS, FL, and XPS spectroscopy. In addition, the photocatalytic activities of $BiVO_4$–graphene composites with different amounts of graphene were discussed. The experimental results had confirmed that $BiVO_4$–graphene composite possessed a relatively high level of photocatalytic activity under visible light irradiation, which might have a wide range of applications in photocatalytic field. The increase in the photocatalytic degradation efficiency could be attributed to graphene which acted as a charge acceptor to promote the separation and transfer of photogenerated carrier.

Acknowledgments

This work was supported by the National Natural Science Foundation of China (21476052, 51172099 and 21271087), the Foundation of Enterprise-University-Research Institute Cooperation from Guangdong Province and the Ministry of Education of China (2013B090600148), and the Science and technology innovation platform project of Foshan City (2014AG100171).

References

[1] J. Ren, W. Wang, M. Shang, S. Sun, E. Gao, Hetero-structured bismuth molybdate composite: Preparation and improved photocatalytic activity under visible-light irradiation, ACS Appl. Mater. Interfaces 3 (2011) 2529–2533.

[2] O. Legrini, E. Oliveros, A.M. Braun, Photochemical processes for water treatment, Chem. Rev. 93 (1993) 671–698.

[3] L. Ge, Novel visible-light-driven $Pt/BiVO_4$ photocatalyst for efficient degradation of methyl orange, J. Mol. Catal. A: Chem. 282 (2008) 62–66.

[4] Y. Shen, M. Huang, Y. Huang, J. Lin, J. Wu, The synthesis of bismuth vanadate powders and their photocatalytic properties under visible light irradiation, J. Alloys Compd. 496 (2010) 287–292.

[5] L. Ge, Synthesis and characterization of novel visible-light-driven $Pd/BiVO_4$ composite photocatalysts, Mater. Lett. 62 (2008) 926–928.

[6] L. Zhang, D. Chen, X. Jiao, Monoclinic structured $BiVO_4$ nanosheets: Hydrothermal preparation, formation mechanism, and coloristic and photocatalytic properties, J. Phys. Chem. B 110 (2006) 2668–2673.

[7] Y. Sun, Y. Xie, C. Wu, S. Zhang, S. Jiang, Aqueous synthesis of mesostructured $BiVO_4$ quantum tubes with excellent dual response to visible light and temperature, Nano Res. 3 (2010) 620–631.

[8] D.K. Lee, I.S. Cho, S. Lee, S.T. Bae, J.H. Noh, D.W. Kim, K.S. Hong, Effects of carbon content on the photocatalytic activity of $C/BiVO_4$ composites under visible light irradiation, Mater. Chem. Phys. 119 (2010) 106–111.

[9] A. Zhang, J. Zhang, Synthesis and characterization of $Ag/BiVO_4$ composite photocatalyst, Appl. Surf. Sci. 256 (2010) 3224–3227.

[10] A. Zhang, J. Zhang, Characterization and photocatalytic properties of $Au/BiVO_4$ composites, J. Alloys Compd. 491 (2010) 631–635.

[11] M. Long, W. Cai, J. Cai, B. Zhou, X. Chai, Y. Wu, Efficient photocatalytic degradation of phenol over $Co_3O_4/BiVO_4$ composite under visible light irradiation, J. Phys. Chem. B 110 (2006) 20211–20216.

[12] Z.-J. Fan, W. Kai, J. Yan, T. Wei, L.-J. Zhi, J. Feng, Y.-M. Ren, L.-P. Song, F. Wei, Facile synthesis of graphene nanosheets via Fe reduction of exfoliated graphite oxide, ACS Nano. 5 (2011) 191–198.

[13] S. Park, R.S. Ruoff, Chemical methods for the production of graphenes, Nat. Nanotechnol. 4 (2009) 217–224.

[14] A.K. Geim, Graphene: Status and prospects, Science 324 (2009) 1530–1534.

[15] A.A. Balandin, S. Ghosh, W.Z. Bao, I. Calizo, D. Teweldebrhan, F. Miao, C.N. Lau, Superior thermal conductivity of single-layer graphene, Nano Lett. 8 (2008) 902–907.

[16] K.I. Bolotin, K.J. Sikes, Z. Jiang, M. Klima, G. Fudenberg, J. Hone, P. Kim, H.L. Stormer, Ultrahigh electron mobility in suspended graphene, Solid State Commun. 146 (2008) 351–355.

[17] M.D. Stoller, S.J. Park, Y.W. Zhu, J.H. An, R.S. Ruoff, Graphene-based ultracapacitors, Nano Lett. 8 (2008) 3498–3502.

[18] C. Wang, D. Li, C.O. Too, G.G. Wallace, Electrochemical properties of graphene paper electrodes used in lithium batteries, Chem. Mater. 21 (2009) 2604–2606.

[19] C. Shan, H. Yang, J. Song, Direct electrochemistry of glucose oxidase and biosensing for glucose based on graphene, Anal. Chem. 81 (2009) 2378–2382.

[20] Y. Wang, Z. Shi, Y. Huang, Y. Ma, C. Wang, M. Chen, Y. Chen, Supercapacitor devices based on graphene materials, J. Phys. Chem. C 113 (2009) 13103–13107.

[21] Y. Zhang, Z.-R. Tang, X. Fu, Y.-J. Xu, TiO_2−Graphene nanocomposites for gas-phase photocatalytic degradation of volatile aromatic pollutant: Is TiO_2−graphene truly different from other TiO_2−carbon composite materials? ACS Nano. 4 (2010) 7303–7314.
[22] W.S. Hummers, R.E. Offeman, Preparation of graphitic oxide, J. Am. Chem. Soc. 80 (1958) 1339–1339.
[23] D.C. Marcano, D.V. Kosynkin, J.M. Berlin, A. Sinitskii, Z. Sun, A. Slesarev, L.B. Alemany, W. Lu, J.M. Tour, Improved synthesis of graphene oxide, ACS Nano. 4 (2010) 4806–4814.
[24] G. Williams, B. Seger, P.V. Kamat, TiO_2–graphene nanocomposites. UV–assisted photocatalytic reduction of graphene oxide, ACS Nano. 2 (2008) 1487–1491.
[25] H. Zhang, X. Lv, Y. Li, Y. Wang, J. Li, P25-graphene composite as a high performance photocatalyst, ACS Nano. 4 (2010) 380–386.
[26] I.V. Lightcap, T.H. Kosel, P.V. Kamat, Anchoring semiconductor and metal nanoparticles on a two-dimensional catalyst mat. Storing and shuttling electrons with reduced graphene oxide, Nano Lett. 10 (2010) 577–583.
[27] T.N. Lambert, C.A. Chavez, N.S. Bell, C.M. Washburn, D.R. Wheeler, M.T. Brumbach, Large area mosaic films of graphene-titania: Self-assembly at the liquid-air interface and photo-responsive behavior, Nanoscale 3 (2011) 188–191.
[28] Q. Li, B. Guo, J. Yu, J. Ran, B. Zhang, H. Yan, J. Gong, Highly efficient visible-light-driven photocatalytic hydrogen production of CdS-cluster-decorated graphene nanosheets, J. Am. Chem. Soc. 133 (2011) 10878–10884.
[29] Q. Xiang, J. Yu, M. Jaroniec, Preparation and enhanced visible-light photocatalytic H_2-production activity of graphene/C_3N_4 composites, J. Phys. Chem. C 115 (2011) 7355–7363.
[30] Y. Wang, P. Gao, L. Huan, X. Wu, Y. Liu, Graphite oxide: Preparation and removal ability of cationic dyes, Chinese J. Inorg. Chem. 28 (2012) 391–397.
[31] T.-F. Yeh, J.-M. Syu, C. Cheng, T.-H. Chang, H. Teng, Graphite oxide as a photocatalyst for hydrogen production from water, Adv. Funct. Mater. 20 (2010) 2255–2262.
[32] J.B. Liu, H. Wang, S. Wang, H. Yan, Hydrothermal preparation of $BiVO_4$ powders, Mater. Sci. Eng. B 104 (2003) 36–39.
[33] L. Lai, L. Chen, D. Zhan, L. Sun, J. Liu, S.H. Lim, C.K. Poh, Z. Shen, J. Lin, One-step synthesis of NH_2-graphene from *in situ* graphene-oxide reduction and its improved electrochemical properties, Carbon 49 (2011) 3250–3257.
[34] Y. Fu, X. Sun, X. Wang, $BiVO_4$–graphene catalyst and its high photocatalytic performance under visible light irradiation, Mater. Chem. Phys. 131 (2011) 325–330.
[35] L. Huang, H. Wang, Y. Liu, C. Chen, Preparation, characterization and photocatalytic activity of Pt-SiO_2/TiO_2 with core-shell structure, Rare Metal Mater. Eng. 11 (2011) 1901–1905.
[36] H. Tang, H. Berger, P.E. Schmid, F. Lévy, Photoluminescence in TiO_2 anatase single crystals, Solid State Commun. 87 (1993) 847–850.
[37] Y.H. Ng, A. Iwase, A. Kudo, R. Amal, Reducing graphene oxide on a visible-light $BiVO_4$ photocatalyst for an enhanced photoelectrochemical water splitting, J. Phys. Chem. Lett. 1 (2010) 2607–2612.